Antiferromagnetism with spin polarization of GaN-based diluted magnetic semiconductors

J. P. T. Santos, M. Marques, and L. K. Teles
Instituto Tecnológico de Aeronáutica, 12228-900 São José dos Campos, SP, Brazil

L. G. Ferreira
Instituto de Física, Universidade de São Paulo, CP 66318, 05315-970 São Paulo, SP, Brazil
(Received 5 May 2009; revised manuscript received 20 February 2010; published 31 March 2010)

The diluted magnetic semiconductors are promising materials for spintronic applications. Usually one intents to find the ferromagnetic state but recently the antiferromagnetism (AFM) was proposed to have some advantages. In this work, we verify the possibility to obtain spin polarization with an AFM state. In particular, we studied GaN 5% double doped with two different transition metals atoms (Mn and Co or Cr and Ni), forming the $Mn_xCo_{0.056-x}Ga_{0.944}N$ and $Cr_xNi_{0.056-x}Ga_{0.944}N$ quaternary alloys. In order to simulate these systems in a more realistic way, and take into account composition fluctuations, we adapted the generalized quasichemical approach to diluted alloys, which is used in combination with spin density-functional theory. We find that is possible to obtain an AFM ground state up to 70% spin polarization.

DOI: 10.1103/PhysRevB.81.115209 PACS number(s): 75.50.Pp, 61.66.Dk, 71.20.Nr, 71.20.Be

I. INTRODUCTION

To implement the new technology of spintronics, efficient techniques for the injection, manipulation, and detection of spins are necessary, and it is crucial the development of materials with these specific characteristics.[1,2] The class of materials called half metals (HMs) (Refs. 3 and 4) have the properties to be one of the most important spintronic systems because it presents ferromagnetism with 100% spin polarization at the Fermi level (E_F). Among the many potential half-metallic systems, there are the diluted magnetic semiconductors (DMSs), that are formed by transition-metal (TM) low doping into standard semiconductors.[5] The DMS represents an interesting possibility of HM materials because they can combine semiconducting and magnetic properties in the same material, being totally compatible with standard microelectronics. However, in order to produce a DMS with all requirements needed, there are still some difficulties to be overcome. Until now, the main problem is to obtain good reproducibility of a material with room-temperature magnetism and semiconducting properties. Besides, there are intrinsic problems related to the usual ferromagnetic DMS for spintronic applications, as the restriction of spin-polarized current by the domain-wall formation and also that the resultant magnetic field can have a destructive effect on integrated circuits. One straight way to avoid these obstacles is the so-called half-metallic antiferromagnet (HM-AFM) system, suggested for the first time by van Leuken and de Groot[6] in Heusler alloys. HM-AFM are materials with 100% spin polarization but with zero total magnetic moment. Aside from the many other proposals for achieving HM-AFM systems, such as double perovskites[7] and hole-doped perovskite cuprate,[8] we emphasize the work of Akai and Ogura,[9] that propose a more complex DMS formed by a semiconductor doped with two different types of transition metals in order to obtain a half metallicity and an AFM ground state. They predicted, by using *ab initio* calculations, that ZnS doped with Cr and Fe atoms can present at the same time AFM and half metallicity. It is worth to point out that until now, as far as we know, there is no experimental evidence of a HM-AFM material. Then, we could ask: is it really possible to obtain a DMS HM-AFM or at least a DMS AFM with spin polarization? This question cannot be answered by considering only the work of Akai and Ogura. Although their work presents very interesting and promising results, the theoretical model only describe an ideal alloy in which there is a homogeneous distribution of atoms. However, real alloys can present composition fluctuation effects that should be taken into account in order to have a more realistic description of such complex systems. Particularly, statistical effects should be crucial in order to obtain properties comparable with real materials. In addition, the majority of DMS calculations in the literature do not take into account the disorder alloy effects, often providing results for unrealistic ordered systems. Therefore, it is of great interest a complete study of these materials that takes into account statistical effects.

In this work, we follow the proposal of Akai and Ogura studying the possibility to obtain an AFM ground state with spin polarization in a DMS system. However, we considered a theoretical model that includes the statistical effects in a more rigorous way: a combination of first-principles calculations with the generalized quasichemical approach.[10,11] In particular, we consider a system not studied before formed by GaN semiconductor doped with two kinds (A and B) of TM pairs: (i) Mn(d^5s^2) and Co(d^7s^2) or (ii) Cr(d^4s^2) and Ni(d^8s^2). The choice of these specific pairs is based on the model assuming that a HM-AFM state is reachable with half occupation of the d bands originating from TM atoms.[9] However, in the case of III-V semiconductors, each TM atom should also provide three electrons for the covalent bonds with the anion (s^2 plus $1d$ electron). Therefore, in order to have half occupation of these d bands, the initial number of d electrons for the TM pair should be 12. The double doping of TM atoms in GaN was also previously studied by Tandon and collaborators[12] with Cr and Mn in GaN with first-principles calculations but they obtained a ferromagnetic (FM) ground state. It should be mentioned that DMS based on GaN have attracted great attention recently because this system was predicted to present room-temperature ferromagnetism (RT-FM).[13] This RT-FM was verified in some

cases[14–16] but also small temperatures are observed.[17,18] Bonanni *et al.*[19] clearly observed three distinct situations for Fe-doped GaN: (i) the DMS itself, (ii) TM-rich phases from spinodal decomposition, or (iii) precipitates with a structure different from the host. They related the FM above room temperature with case (ii). Nevertheless, this point is still controversial in the literature, and the nitride DMS properties should critically depend on the growth conditions. In this work, we intend to study a DMS as a diluted alloy with no cluster formation, aiming at the possibility of obtaining an antiferromagnetic and half-metallic system based on GaN semiconductor. Aside from the expected higher Curie temperature, there are a large number of technological advantages associated with nitrides[20] and the possibility of implementation of spintronics in wideband-gap semiconductors can provide unique devices.

This paper is organized as follows, in Sec. II, we develop the GQCA formalism applied to diluted systems, also describing the *ab initio* method used for total-energy calculations. In Sec. III, we present the results, first for the properties of ordered structures, followed by GQCA results for the alloys. Finally, in Sec. IV, we present the conclusions of this work.

II. THEORETICAL MODEL

In order to make a theoretical study of the proposed system, we used a statistical model to take into account the disorder of the system by using the generalized quasichemical approach (GQCA) (Ref. 10) combined with spin density-functional theory.[21] The GQCA was already used successfully for the study of several nitride-based ternary and quaternary alloys.[11,22,23] Here we adapted the method in order to study diluted quaternary alloys. In the GQCA method, the alloy is divided into an ensemble of individual clusters statistically and energetically independent of the surrounding atomic configuration. For a particular choice of the supercell used as the basic cluster, there are J different cluster kinds, each one with a degeneracy g_j (equivalent clusters by symmetry). Any property P of interest (total energy, spin polarizations, etc.) of the quaternary alloy $A_xB_yC_{1-x-y}N$, with compositional disorder, can be expressed as

$$P = \sum_{j=1}^{J} P_j x_j(x,y,T), \tag{1}$$

where P_j is the property of the j cluster, and $x_j(x,y,T)$, the central quantity of GQCA method, gives the probability of cluster j occurrence at compositions x and y and growth temperature T. As mentioned before, the GQCA approach to quaternary alloys[11] is here modified and simplified because we assume that the alloy is diluted, that is, we do not consider the possibility of clustering, and studied only low TM content. This fact is introduced in our model by considering supercells with only 72 atoms ($n=36$ cations), and just two substitutional TM in the cation sublattice. In other words, we have the constraint $y=\gamma-x$, with $\gamma=2/n=5.5\%$, so that the alloy has composition $A_xB_{\gamma-x}C_{1-\gamma}D$. This approximation allows the use of a supercell as large as $n=36$, thus describing the magnetic semiconductor in a best way. The probability x_j is obtained by finding the minimum free energy F, by using the Lagrange multipliers formalism with the constraints $\Sigma_{j=1}^{J} x_j=1$, for the probability, and $\Sigma_{j=1}^{J} n_j x_j=nx$ for the composition. In these circumstances, x_j can be expressed as

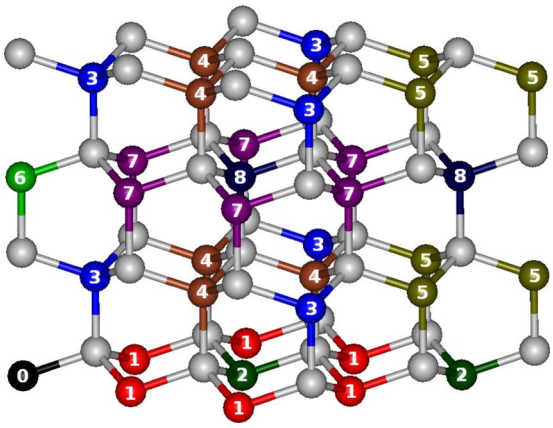

FIG. 1. (Color online) Schematic positions of 72-atom supercell used in the calculations. The numbered spheres are Ga positions and the empty spheres are N. The first transition-metal atom (a) is fixed in the position 0 and the second (b) is located in one of the other positions (1 to 8), giving in the end 8 positional configurations.

$$x_j(x,T) = \frac{g_j \eta^{n_j} e^{-E_j/k_BT}}{\sum_{j'=1}^{J} g_{j'} \eta^{n_{j'}} e^{-E_{j'}/k_BT}}, \tag{2}$$

where k_B is the Boltzmann constant, n_j and E_j are the number of A atoms (0, 1, or 2) and the total energy, respectively, for the cluster j. The η parameter is obtained solving the simple second-order polynomial equation,

$$c_2\eta^2 + c_1\eta + c_0 = 0, \tag{3}$$

where the coefficients c_k are given by

$$c_k = \sum_{j=1}^{J} \delta_{kn_j} g_j (nx - n_j) e^{-E_j/k_BT} \tag{4}$$

with δ_{kn_j} equal 1 for $k=n_j$ and 0 for $k \neq n_j$.

We considered the wurtzite structure, with the commom lattice parameters a and c, by using a supercell with 72 atoms, $3a \times 3a \times 2c$, as shown in Fig. 1, where we also show the eight nonequivalent positions for the TM pairs (positional configurations). In Table I, we present the degeneracy and the distance between TM atoms for each configuration. One sees that the distance between the TM varies in a broad range, from 3 to 7 Å. The TM atoms can be equal (A-A or B-B), or different (A-B), leading to 24 configurations. Further, the TMs may have spins in the same or in the opposite direction, corresponding to a FM or an AFM state of the $A_xB_{0.055-x}Ga_{0.945}N$ alloy. Thus, in the FM case, we have 24 different clusters with A-A, B-B, and A-B coupling ferromagnetically, and E_j in the Eqs. (2) and (4) are equal to E_j^{FM}, with which it will be obtained a x_j^{FM}, and consequently all the properties P.

TABLE I. Degeneracy g_j and distance between TM atoms for the eight positional configurations.

Configuration	g_j	Distance (Å)
1	6	3.22
2	2	5.58
3	6	3.20
4	6	5.57
5	6	4.54
6	1	5.22
7	6	6.13
8	2	7.64

In the same way, the AFM state is simulated with clusters in which the TM atoms A and B have opposite spins, leading to all AFM properties. Note that this is the simplest AFM arrangement of interactions possible because the compensation of magnetic moments is obtained only by pairs. Any other AFM configuration would imply in at least four-atoms' interactions. However, in a disordered diluted system, the statistics of low-concentration impurities is much unfavorable to four atoms to be close enough for a significant magnetic interaction. Therefore, although exists much more complex AFM arrangement of spins, they should be very unlikely. Complementarily, we made a simple test calculation of four-atoms AFM interactions. The configuration used presents two Mn spin-up atoms in positions 0 and 1, and two Co spin-down atoms in positions 6 and 7 (Fig. 1). We verified that this AFM four-atom interaction is not stable, resulting in a ferrimagnetic state with a total magnetic moment of about $2.0\mu_B$. However, if we fix the total magnetic moment to be zero, we obtain an AFM state with null spin polarization. Also, this configuration is less energetically favorable compared with a configuration with the atoms in the same position but with Mn(up)-Mn(down) and Co(up)-Co(down) magnetic interactions (which corresponds to the used AFM configuration based on pairs). Concluding, these conjectures and results are consistent indications that the AFM pair-based configuration used is suitable to describe the studied system.

The composition of 5.5% TM is suitable to simulate the usual concentrations used in experimental samples of DMS based on GaN.[5] The input parameters for the GQCA method were obtained by using the density-functional calculations within the generalized gradient approximation for the exchange-correlation potential.[24] The local spin-density approximation[25] was also tested, leading to the same main conclusions. For the resolution of Kohn-Sham equations, we worked with projector-augmented wave method[26] as implemented in the VASP code,[27] with $3\times3\times3$ k points in the Brillouin zone and a cutoff energy of 282.67 eV. All atomic coordinates in the supercell are relaxed until the Hellmann-Feynman forces vanish, using as the criterion that the energy difference between two successive changes in atomic positions is $\leq 10^{-4}$ eV. It was verified that the lattice parameters we obtained for GaN, $a=3.22$ Å and $c=5.25$ Å, were significantly not affected by the substitution of two Ga atoms with TM atoms, thus these values were considered in all calculations.

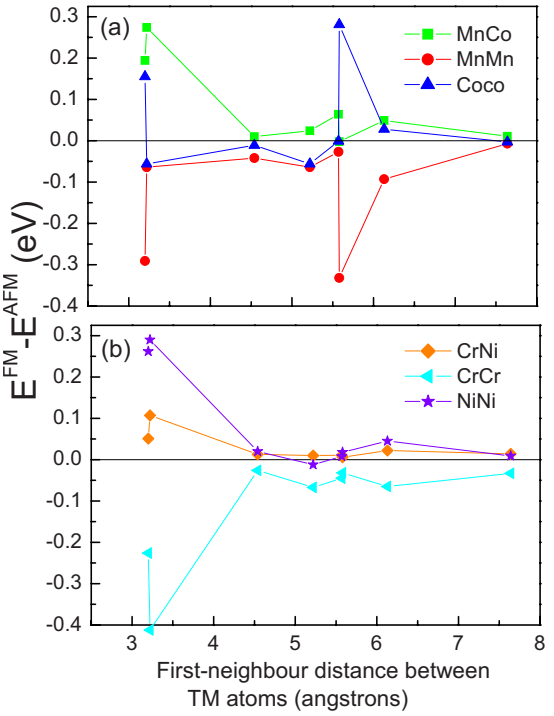

FIG. 2. (Color online) Total-energy difference between FM and AFM states versus first-neighbor distance for (a) MnCoGaN alloy configurations with Mn-Mn, Co-Co, and Mn-Co interactions and (b) CrNiGaN alloy configurations with Cr-Cr, Ni-Ni, and Cr-Ni interactions.

III. RESULTS AND DISCUSSION

The GQCA model in combination with these 72-atom configurations allow us to simulate realistic concentrations of TM atoms in GaN and also include disorder effects of the ABGaN (A and B=TM) quaternary alloy because it is possible to take into account two kinds of first neighborhood for each TM atom A: A-A or A-B. This fact is very important because, as we shall see, the electronic properties of A-B configurations are completely different from those of A-A or B-B configuration. Of course in a real random alloy, both cases will happen. In Fig. 2, we present the results for the difference between total energy for FM and AFM states. In the case (a) for the MnCoGaN configurations, we can see that Mn-Co have mainly AFM coupling while for pure Mn configurations, we have FM coupling. For the Co-Co configurations, there is a oscillatory behavior between FM and AFM states. In the case of the CrNiGaN alloys, the behavior is different. The Cr-Ni and Ni-Ni configurations have an AFM ground state. Cr-Cr configurations, however, are FM. Therefore, we expect a transition from an AFM to FM ground state increasing the amount of Mn or Cr in the alloys. As a main tendency, the magnetic interaction rapidly decreases with the distance between TM atoms. However, other effects such as second neighbors, number of neighbors, and

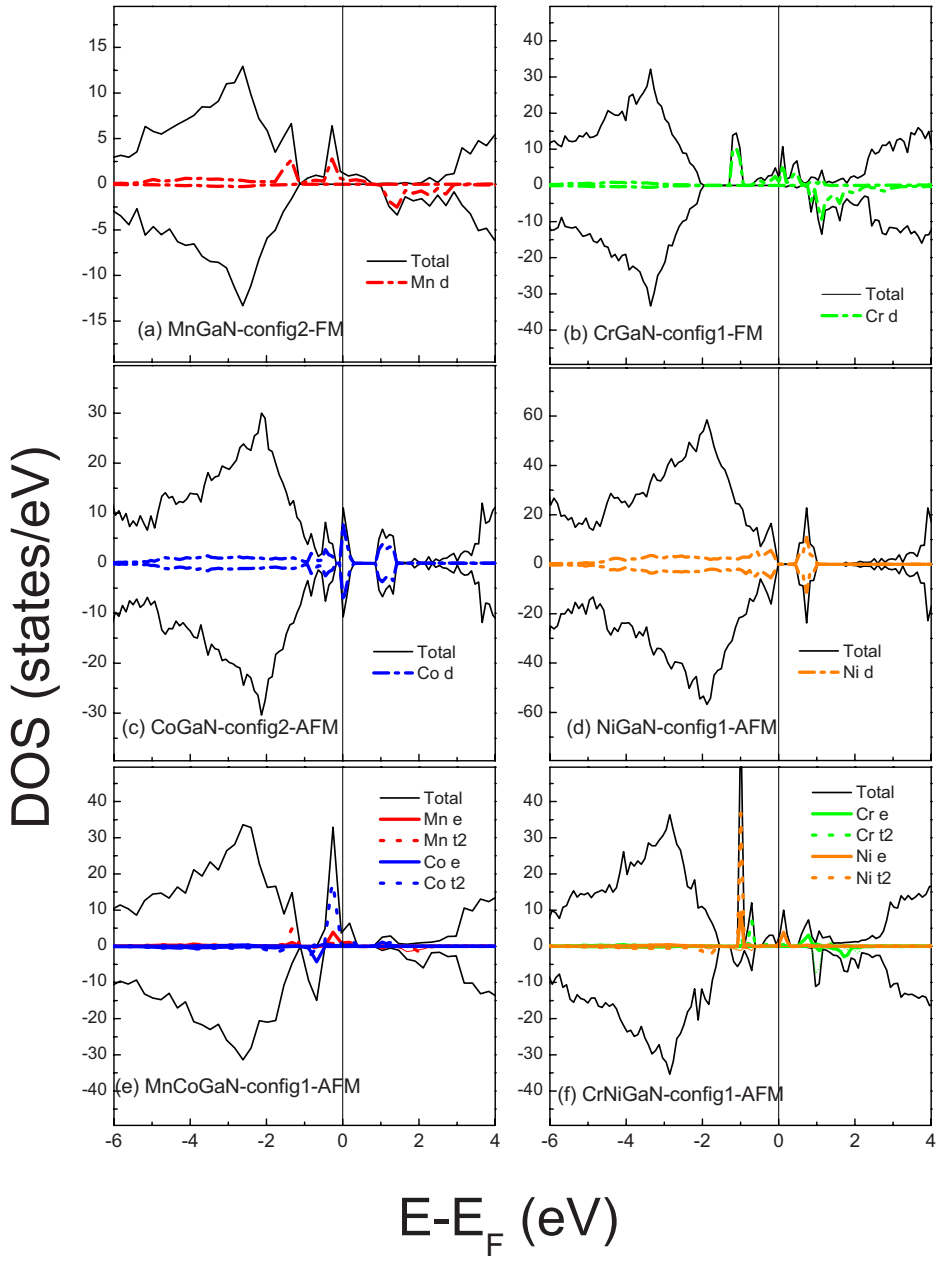

FIG. 3. (Color online) Density of states versus energy of the lowest total-energy configuration for six different dopings: (a) Mn-Mn, (b) Cr-Cr, (c) Co-Co, (d) Ni-Ni, (e) Mn-Co, and (f) Cr-Ni. The projected density of states of *d* orbital of each TM is also presented, and, in the cases of (e) Mn-Co and (f) Cr-Ni, these contributions are still separated in *e* and *t*2 states. Positive values mean spin-up states and negative values mean down states.

direction of interactions are responsible for some deviations from this behavior, specially in the case of MnCoGaN where strong magnetic couplings are obtained even for an intermediate value of the distance between TM atoms in the cell. The results for Cr-Cr and Mn-Mn magnetic interactions can be compared with previous results obtained by Cui *et al.*[28,29] In the mentioned papers, there are results using the same cell that we used for Cr and Mn doping of GaN: (i) the results for Mn doping in GaN (Ref. 29) are in good agreement with us; the ground state is FM in all configurations and in general way, the energy difference between FM and AFM states decrease strongly with the distance; and (ii) the results for Cr doping, although also show a very fast decay of the total-energy difference between FM and AFM states,[28] similar with our result, there is a oscillatory behavior in the ground state of the configurations between FM and AFM states. In our case, Cr-doping GaN is always FM as already showed.

The total and partial (for *d* orbital of TM atoms) density of states (DOS) for the six different types of configurations (Mn-Co, Mn-Mn, Co-Co, Cr-Ni, Cr-Cr, and Ni-Ni) are presented in Fig. 3. For each type of configuration, there are 16 possible choices (8 positional times 2 magnetic). We only present the configurations with smaller total energy.

We find: (i) *general aspects*: as a general behavior of TM atoms in GaN, we verified that the *d* bands are always around the Fermi energy, that is located inside the energy-

gap region. Because of the crystal symmetry, these *d* states of TM atoms are separated in *e* and *t*2 levels. There is a small hybridization of these states with valence band, which is almost nonpolarized. This behavior is very different from the MnGaAs standard DMS in which there occurs a significant spin polarization of the valence band.[30] If we exclude the TM *d* bands, the DOS is like the one of GaN, meaning that the systems keep the semiconducting character.

(ii) *DOS of ternary alloys (A-A or B-B configurations)*: for MnGaN and CrGaN, the ground state is FM. For MnGaN [Fig. 3(a)], the majority of *d* states is inside the energy gap, with a small hybridization with N *p* states, leading also to a small change in valence-band maximum region. However, for CrGaN alloy [Fig. 3(b)], there occurs the formation of deeper acceptor bands, localized about 1 eV above valence-band maximum (VBM) with negligible perturbation on the GaN valence band. In both cases, we have a spin-polarized impurity band for most states, with the Fermi energy running through it, and a band gap of about 2 eV in the minority-spin channel. For CoGaN and NiGaN [Figs. 3(c) and 3(d)], the ground state is AFM with null spin polarization. The hybridization of *d* states with VBM are larger in comparison to the CrGaN and MnGaN whereas the hybridization with the conduction band is negligible. For CoGaN, the Fermi energy cuts the band, providing free carriers. On the other hand, for NiGaN, the Fermi energy lies in the energy gap.

(iii) *DOS of quaternary alloys (A-B configurations)*: the results are depicted in Figs. 3(e) and 3(f). We can observe that the systems present 100% spin polarization and are half metallic for both double doping types, as in the CrGaN and MnGaN cases but these aspects occurred now for an AFM ground state. This behavior can be explained based on the separation of the *d* bands of atoms *A* and atoms *B* and the Zeeman splitting between spin-up and spin-down states. In Fig. 4, we present schematically how this effect can occur. The FM and AFM coupling between the different TM atoms *A* and *B* are represented, respectively, in Figs. 4(a) and 4(b). The separation between its *d* bands is indicated by Δ_d and the Zeeman splitting by Δ_Z. For simplicity, Δ_Z is taken to be equal for *A* and *B* atoms, i.e., $\Delta_Z^A = \Delta_Z^B$. The conditions for the occurrence of half metallicity with an AFM state are: (i) the energy positions of the *d* bands of atoms *A* and atoms *B* do not coincide ($\Delta_d \neq 0$), (ii) the magnetic coupling between them is AFM, and (iii) there is the splitting between spin-up and spin-down *d* bands ($\Delta_Z \neq 0$). Besides these conditions, the HM-AFM ground state is only reached because the values of Δ_d and Δ_Z are high enough in such a way that the Fermi energy for spin up lies on the band and for spin down lies on the gap, and there is a full compensation of density of states (*D*) for spin up (↑) and spin down (↓) [$\int_{-\infty}^{E_F} D^{\uparrow}(E)dE = \int_{-\infty}^{E_F} D^{\downarrow}(E)dE$]. Note that in Fig. 4(b), the sum of occupied spin-up states of TM *A* and *B* is equal to the spin down of TM *A*. Fortunately, this is the case for the two kinds of doping that we studied. Returning to Fig. 3, we can see that in the Fermi energy, the polarized band is mainly the combination of *t*2 state of Co and *e* state of Mn in the MnCoGaN alloy but is only the *e* state of Ni for the CrNiGaN alloy. The dispersion of the polarized band is higher for MnCoGan alloy than CrNiGaN alloy, indicating that the first one should present better transport properties.

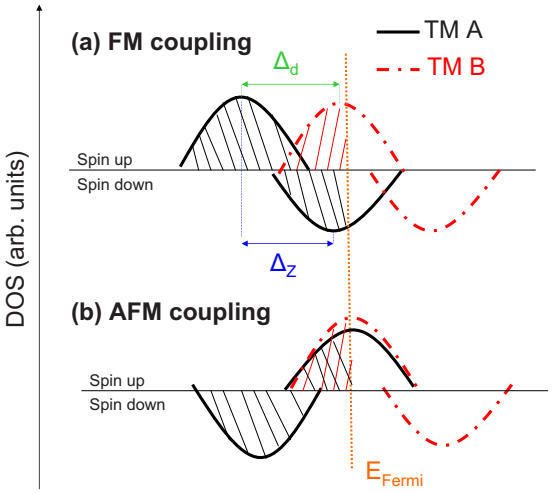

FIG. 4. (Color online) Schematic representation of the density of states of *d* orbital for (a) FM and (b) AFM coupling between *A* and *B* TM atoms in GaN host. Δ_d is the separation between different *d* bands and Δ_Z is the Zeeman splitting between spin-down and spin-up states, which is taken for simplicity to be equal for TM *A* and TM *B*. In the case of (b) AFM, we assume compensation of spins up and down: $\int_{-\infty}^{E_F} D^{\uparrow}(E)dE = \int_{-\infty}^{E_F} D^{\downarrow}(E)dE$

(iv) *Comparison among the DOS*: for quaternary alloys, the minority-spin gap is decreased in both cases if we compare with the ternaries MnGaN and CrGaN. While MnCoGaN maintains the same hybridization with the valence band as the ternary MnGaN, CrNiGaN and the ternary CrGaN do not present any important hybridization.

In Table II, we present the results for local magnetic moments of all eight Co-Mn configurations. A proper choice of TMs (such as Mn-Co or Cr-Ni) results in the same number of *d* electrons in each spin direction thus making possible the AFM coupling.[9] Nevertheless, locally the magnetic moment of Co (Ni) does not compensate the local magnetic moment of Mn (Cr) in the AFM ground state. In the Mn-Co case, the Co atom has about 85% of magnetic moment of Mn atom (with a similar result also for Cr-Ni configurations). What happens is that the N atoms bonded with Co are significantly polarized. The spin polarization of the N atoms can also be observed in Fig. 5, which presents the density of states of the

TABLE II. Local magnetic moments for Mn, Co, and N first neighbors of Co (average value), and N first neighbors of Mn (average value) for the eight Co-Mn AFM configurations. The other N atoms do not present significant spin polarizations.

Configuration	$\mu_{Mn}(\mu_B)$	$\mu_{Co}(\mu_B)$	$\mu_N(\mu_B)$-Mn	$\mu_N(\mu_B)$-Co
1	3.065	−2.493	0.037	−0.098
2	3.035	−2.813	0.020	−0.098
3	3.083	−2.505	0.035	−0.100
4	3.323	−2.676	0.007	−0.102
5	3.332	−2.728	0.010	−0.099
6	3.280	−2.818	0.009	−0.095
7	3.280	−2.646	0.005	−0.099
8	3.700	−3.185	0.030	−0.111

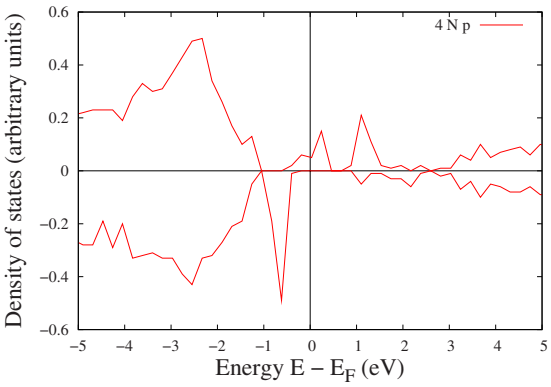

FIG. 5. (Color online) *p*-orbital projected density of states of four N first neighbors of Co in MnCoGaN configuration 1. Positive values mean spin-up states and negative values mean down states.

N-atom *p* orbitals that are first neighbors to the Co atom in MnCoGaN configuration 1. Therefore, the magnetic moment of Mn (Cr) is compensated by the magnetic moment of the Co(Ni)-N cluster.

In Table III, we present the values for spin polarizations for *A*-*B* configurations. For each configuration, we calculate the spin polarization by the simple definition,

$$Pol = \frac{N_\uparrow - N_\downarrow}{N_\uparrow + N_\downarrow}, \tag{5}$$

where N is the density of states at Fermi energy for spin up ($\uparrow$) or spin down ($\downarrow$), calculated in very precise DOS calculations. We also verified that the half metallicity happens for all *A*-*B* configurations in the AFM state. By symmetry, the spin polarization of *A*-*A* and *B*-*B* AFM configurations is always zero, a result that was verified in the calculations. For the FM calculations, the spin polarizations of *A*-*B* configurations present long-range variations, from very small to 100%, reinforcing the necessity of taking into account a statistical method to treat these diluted alloys. Finally, *A*-*A* or *B*-*B* FM configurations, in most cases, have 100% spin polarization.

TABLE III. Spin Polarization for *A*-*B* configurations. For configurations *A*-*A* and *B*-*B*, the polarizations is always 0 for the FM state and 100% for the AFM state.

	Spin polarizations (%)			
Configuration	MnCo-AFM	MnCo-FM	CrNi-AFM	CrNi-FM
1	100	40	100	24
2	100	18	100	100
3	100	100	100	45
4	100	10	100	100
5	100	18	100	0
6	100	30	100	86
7	100	12	100	100
8	100	20	100	100

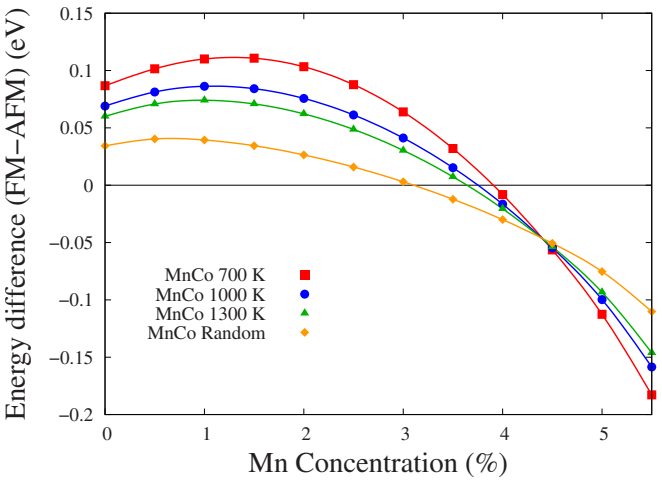

FIG. 6. (Color online) GQCA total-energy difference between FM and AFM states versus concentration x for the $Mn_xCo_{0.056-x}Ga_{0.944}N$ alloy at the growth temperatures 700, 100, and 1330 K, and also for the random distribution of atoms.

From this point on, we will present GQCA results for $Mn_xCo_{0.056-x}Ga_{0.944}N$ and $Cr_xNi_{0.056-x}Ga_{0.944}N$ alloys calculated assuming FM or AFM coupling of spins. These results are presented in the whole range of compositions (x from 0 to 0.055) and with the growth temperatures of 700, 1000, and 1300 K that are representative of typical samples of GaN-based DMS in the literature. We also include results for the random distribution of atoms. In Figs. 6 and 7, it is presented the GQCA total-energy difference between FM and AFM states versus the TM compositions. We can see that the systems present the desired AFM ground state until 3.7% Mn in the case of $Mn_xCo_{0.056-x}Ga_{0.944}N$ alloy and until 3.3% in the case of $Cr_xNi_{0.056-x}Ga_{0.944}N$ alloy. Therefore, $Cr_{0.056}Ga_{0.944}N$ and $Mn_{0.056}Ga_{0.944}N$ present a FM ground state and $Co_{0.056}Ga_{0.944}N$ and $Ni_{0.056}Ga_{0.944}N$ present an AFM ground state. The explanation for these magnetic transitions is simple. It happens because Mn-Co (Cr-Ni) and also Co-Co

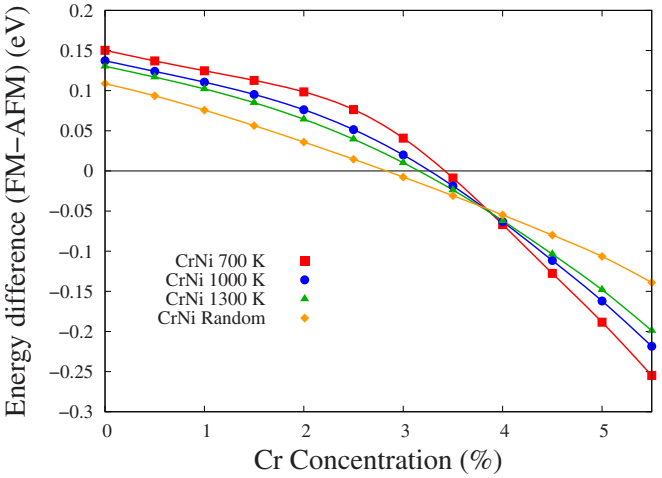

FIG. 7. (Color online) GQCA total-energy difference between FM and AFM states versus concentration x for the $Cr_xNi_{0.056-x}Ga_{0.944}N$ alloy at the growth temperatures 700, 100, and 1330 K, and also for the random distribution of atoms.

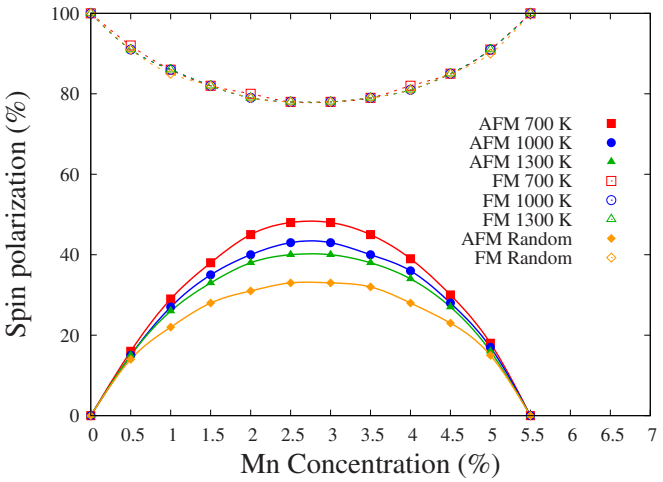

FIG. 8. (Color online) GQCA spin polarization for FM and AFM states versus concentration x for the $Mn_xCo_{0.056-x}Ga_{0.944}N$ alloy at the growth temperatures 700, 100, and 1330 K, and also for the random distribution of atoms.

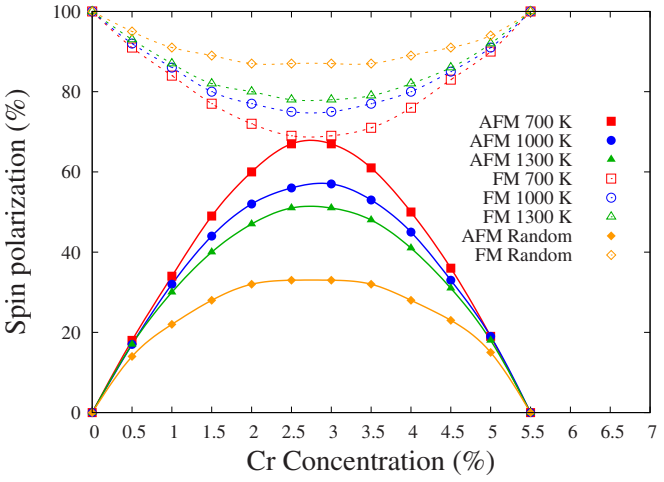

FIG. 9. (Color online) GQCA spin polarization for FM and AFM states versus concentration x for the $Cr_xNi_{0.056-x}Ga_{0.944}N$ alloy at the growth temperatures 700, 100, and 1330 K, and also for the random distribution of atoms.

(Ni-Ni) first-neighbors interactions are essentially AFM while Mn-Mn (Cr-Cr) have FM coupling, as already shown in Fig. 2. The effect of the growth temperature is small, with the FM-AFM energy difference being higher for small growth temperatures (far from random distribution), because the configurations with small distance between TM have higher probability x_j. The larger difference between FM and AFM states occurred at about 1% Mn for the AFM ground state for the quaternary MnCoGaN alloy. However, for FM ground states and also CrNiGaN AFM ground-state regions, the larger energy difference occurred in the limit of the respective ternary compounds. Therefore, it is clear that there is a large composition range of AFM ground states for the two quaternary alloys.

In Figs. 8 and 9, we present the Eq. (5) spin polarization as a function of composition and growth temperature. We can see that for all ternary alloys MnGaN, CoGaN, CrGaN, and NiGaN (for 0 or 5.5% composition in our model), we have a half-metallic state with 100% polarization for the FM state, which is decreased when the quaternary alloy is formed. However, for the AFM state, the polarization is zero in the extremes due to the symmetry but a nonzero polarization appears in the quaternary region of concentration with its maximum value occurring for equal composition of the two transition-metal atoms. The growth temperature effect is more intense in the case of CrNiGaN quaternary alloy, with a spin polarization of about 70% at 700 K which decays to about 30% when reaching the random distribution of infinite temperature. In the MnCoGaN case, we have a maximum of 45% spin polarization. The enhancement of the spin polarization as the growth temperature decreases reveals that the formation of Cr-Ni or Mn-Co pair is more stable than a quaternary alloy formed by two separated ternary alloys (MnGaN and CoGaN or CrGaN and NiGaN).

Finally, in Fig. 10, we present the results for magnetic critical transition temperature T_c (Curie temperature in the case of FM ground state and Néel temperature for an AFM ground state). The critical temperature of the alloys is obtained within the GQCA formalism as

$$T_C = \sum_{j=1}^{J} x_j(x,T) T_C^j, \tag{6}$$

where the transition magnetic temperature of each cluster (T_C^j) are roughly estimated using the mean-field approximation (MFA). Considering that for all configurations, the magnetic interactions for the AFM case are always between different spins, we obtain the simple expression for T_C^j,

$$T_C^j = \frac{1}{2}\frac{|E_{\mathrm{FM}} - E_{\mathrm{AFM}}|}{k_B}. \tag{7}$$

The difference between total energies for FM and AFM states is taken in modulus because the expression is being used for both FM and AFM cases. It is well known that the overestimation of T_c by the MFA but our main goal here is to

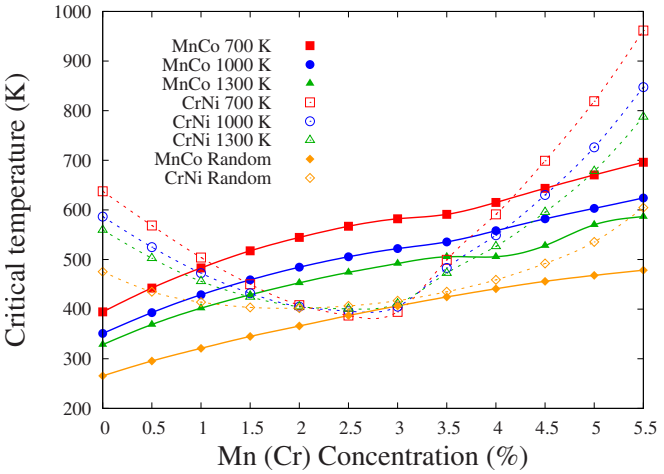

FIG. 10. (Color online) Magnetic transition temperature versus concentration x for $Mn_xCo_{0.056-x}Ga_{0.944}N$ and $Cr_xNi_{0.056-x}Ga_{0.944}N$ alloys for the growth temperatures 700, 100, and 1330 K, and also for the random distribution of atoms.

compare T_c for the ternary and quaternary alloys that we studied, in all composition range and growth temperature conditions. The general T_c of the alloy for a composition x and growth temperature T is obtained by using Eq. (7) and is presented in Fig. 10. The highest T_c, comparing two different dopings, is obtained in the limit of the CrGaN ternary, with the other limit NiGaN also presenting high T_c. Clearly, T_c decreases with the formation of quaternary CrNiGaN alloy with a minimum value at about the same composition of Cr and Ni. However, for the MnCoGaN case, there is an approximately linear transition between the smaller value of CoGaN and higher value of MnGaN alloy. Here, the effect of growth temperature is small in the CrNiGaN system and very significant in the case of MnCoGaN with a difference of about 200 K between a growth temperature of 700 K and a random distribution of TM atoms. Our results indicate that these systems present higher critical magnetic temperatures when we have a FM than an AFM ground state. The GQCA results show that the AFM state is more stable for small value of x but the maximum polarization is obtained for equal compositions of two different TM atoms. However, the critical transition magnetic temperatures decreases for small x in the case of MnCoGaN alloy but increases for small x in the case of CrNiGaN alloy. Therefore, an optimized composition should be obtained in each quaternary case in order to have a system with a stable antiferromagnetism and high values of T_c and spin polarization.

IV. CONCLUSIONS

In conclusion, we found that the magnetic couplings of the TM pairs Co-Mn and Cr-Ni are antiferromagnetic in GaN host. Also, the formation of these pairs (Mn-Co and Cr-Ni) is more stable than the separation of these same atoms in mutual Mn-Mn and Co-Co pairs (or Cr-Cr and Ni-Ni pairs). In an ordered structure, only containing Mn-Co (or Cr-Ni) magnetic interactions the ground state besides being AFM, has 100% spin polarization, forming the so-called AFM half metals. However, including statistical effects with the GQCA method in order to simulate the $Mn_xCo_{0.056-x}Ga_{0.944}N$ and $Cr_xNi_{0.056-x}Ga_{0.944}N$ quaternary diluted magnetic semiconductors alloys, we obtained an AFM ground state until only about $x=0.035$. The half metallicity is lost by the presence of Mn-Mn and Co-Co (or Cr-Cr and Ni-Ni) pairs but still there is significant spin polarization (about 70% in our best case). Finally, with a simple model, but also with the inclusion of disorder effects, we compare transition magnetic temperatures for the different systems. With the same transition-metal composition (about 5.5%), we obtained that the quaternary CrNiGaN system should have smaller T_C than the respective ternaries alloys CrGaN and NiGaN. Otherwise, MnCoGaN should have an intermediate T_C between MnCoN (smaller) and MnGaN (higher). The optimized condition for higher values of spin polarization and transition magnetic temperature are 2.5% Mn and 2.5% Co in the MnCoGaN system, and 1.5% Cr ad 3.5% Ni in the CrNiGaN system.

[1] S. A. Wolf, D. D. Awshalom, R. A. Buhrman, J. M. Daughton, S. von Molnár, M. L. Roukes, A. Y. Chtchelkanova, and D. M. Treger, Science **294**, 1488 (2001).

[2] I. Žutić, J. Fabian, and S. D. Sarma, Rev. Mod. Phys. **76**, 323 (2004).

[3] W. E. Pickett and J. S. Moodera, Phys. Today **54**(5), 39 (2001).

[4] M. I. Katsnelson, V. Yu. Irkhin, L. Chioncel, A. I. Lichtenstein, and R. A. de Groot, Rev. Mod. Phys. **80**, 315 (2008).

[5] T. Jungwirth, J. Sinova, J. Masek, J. Kucera, and A. H. MacDonald, Rev. Mod. Phys. **78**, 809 (2006).

[6] H. van Leuken and R. A. de Groot, Phys. Rev. Lett. **74**, 1171 (1995).

[7] W. E. Pickett, Phys. Rev. B **57**, 10613 (1998).

[8] Y. M. Nie and X. Hu, Phys. Rev. Lett. **100**, 117203 (2008).

[9] H. Akai and M. Ogura, Phys. Rev. Lett. **97**, 026401 (2006).

[10] A.-B. Chen and A. Sher, *Semiconductor Alloys* (Plenum Press, New York, 1995).

[11] M. Marques, L. K. Teles, L. G. Ferreira, L. M. R. Scolfaro, J. Furthmuller, and F. Bechstedt, Phys. Rev. B **73**, 235205 (2006).

[12] N. Tandon, G. P. Das, and A. Kshirsagar, Phys. Rev. B **77**, 205206 (2008).

[13] T. Dietl, H. Ohno, F. Matsukura, J. Cibert, and D. Ferrand, Science **287**, 1019 (2000).

[14] H. Hori, S. Sonoba, T. Sasaki, Y. Yamamoto, S. Shimizu, K. Suga, and K. Kindo, Physica B **324**, 142 (2002).

[15] M. L. Reed, N. A. El-Masry, H. H. Stadelmaier, M. K. Ritums, M. J. Reed, C. A. Parker, J. C. Roberts, and S. M. Bedair, Appl. Phys. Lett. **79**, 3473 (2001).

[16] P. P. Chen, H. Makino, J. J. Kim, and T. Yao, J. Cryst. Growth **251**, 331 (2003).

[17] M. E. Overberg, C. R. Abernathy, S. J. Pearton, N. A. Theodoropoulou, K. T. McCarthy, and A. F. Hebard, Appl. Phys. Lett. **79**, 1312 (2001).

[18] N. Theodoropoulou, A. F. Hebard, M. E. Overberg, C. R. Abernathy, S. J. Pearton, S. N. G. Chu, and R. G. Wilson, Appl. Phys. Lett. **78**, 3475 (2001).

[19] A. Bonanni, A. Navarro-Quezada, T. Li, M. Wegscheider, Z. Matej, V. Holy, R. T. Lechner, G. Bauer, M. Rovezzi, F. D'Acapito, M. Kiecana, M. Sawicki, and T. Dietl, Phys. Rev. Lett. **101**, 135502 (2008).

[20] S. J. Pearton, C. R. Abernathy, G. T. Thaler, R. M. Frazier, D. P. Norton, F. Ren, Y. D. Park, J. M. Zavada, I. A. Buyanova, W. M. Chen, and A. F. Rebard, J. Phys.: Condens. Matter **16**, R209 (2004).

[21] P. Hohenberg and W. Kohn, Phys. Rev. **136**, B864 (1964).

[22] M. Marques, L. K. Teles, L. M. R. Scolfaro, J. R. Leite, J. Furthmüller, and F. Bechstedt, Appl. Phys. Lett. **83**, 890 (2003).

[23] C. Caetano, L. K. Teles, M. Marques, A. Dal Pino, Jr., and L. G. Ferreira, Phys. Rev. B **74**, 045215 (2006).

[24] Y. Wang and J. P. Perdew, Phys. Rev. B **43**, 8911 (1991).

[25] D. M. Ceperley and B. J. Alder, Phys. Rev. Lett. **45**, 566 (1980); J. P. Perdew and A. Zunger, Phys. Rev. B **23**, 5048 (1981).

[26] G. Kresse and D. Joubert, Phys. Rev. B **59**, 1758 (1999).

[27] G. Kresse and J. Furthmüller, Comput. Mater. Sci. **6**, 15 (1996); Phys. Rev. B **54**, 11169 (1996).

[28] X. Y. Cui, J. E. Medvedeva, B. Delley, A. J. Freeman, and C. Stampfl, Phys. Rev. B **75**, 155205 (2007).

[29] X. Y. Cui, B. Delley, A. J. Freeman, and C. Stampfl, Phys. Rev. B **76**, 045201 (2007).

[30] J. M. D. Coey and S. Sanvito, J. Phys. D **37**, 988 (2004).